Check for updates

Climate change and its implications for rainfed agriculture in Ethiopia

Desalew Meseret Moges and H. Gangadhara Bhat

ABSTRACT

This study aims to investigate the spatio-temporal variability and trends in climate and its implications for rainfed agriculture in the Rib watershed, north-western highland Ethiopia from 1986 to 2050. The daily rainfall and temperature records for the period 1986–2017 were used to detect the variability and trends of the current climate using the coefficient of variation, precipitation concentration index, Mann–Kendall test, and Sen's slope estimator. On the other hand, future climate changes (2018–2050) were analyzed based on the Coupled Model Intercomparison Project version 5 (CMIP5) model outputs under under two representative concentration pathway (RCP) scenarios, RCP 4.5 and 8.5. The results showed high inter-seasonal and inter-annual variability of rainfall and temperature in the studied watershed over the last four decades. The annual and *Kiremt* (June–September) rainfall showed a generally increasing trend, while the *Belg* (March–May) rainfall exhibited a decreasing trend between 1986 and 2017. Conversely, the minimum, maximum and mean temperature demonstrated increasing trends over the study period although most of the detected trends were statistically insignificant at 5 and 10% level of significance. Future climate analysis results showed an increase in future temperature and annual and *Kiremt* rainfall while *Belg* rainfall declined.

Key words | climate projections, Mann–Kendall test, rainfall and temperature, rain-fed agriculture

HIGHLIGHTS

- Both the current and future rainfall and temperature changes and variability were analysed.
- Five CMIP5 model outputs and two emission scenarios were considered for analysis of future climate.
- Mapping the spatial distribution of rainfall and PCI is essential for water use planning and policy making.
- Evaluation of seasonal climate variability and change is vital for rain-fed agriculture, particularly in developing countries like Ethiopia.
- Mann-Kendall test and coefficient of variation were found to be important techniques for analysis of climate variability and trends.

Desalew Meseret Moges (corresponding author)
Department of Geoinformatics,
Mangalore University,
Mangalagangotri 574199, Mangalore,
India
E-mail: *mdessalew@gmail.com*

H. Gangadhara Bhat
Department of Marine Geology,
Mangalore University,
Mangalagangotri 574199, Mangalore,
India

This is an Open Access article distributed under the terms of the Creative Commons Attribution Licence (CC BY 4.0), which permits copying, adaptation and redistribution, provided the original work is properly cited (http://creativecommons.org/licenses/by/4.0/).

doi: 10.2166/wcc.2020.058

Downloaded from http://iwa.silverchair.com/jwcc/article-pdf/12/4/1229/896416/jwc0121229.pdf
by guest

GRAPHICAL ABSTRACT

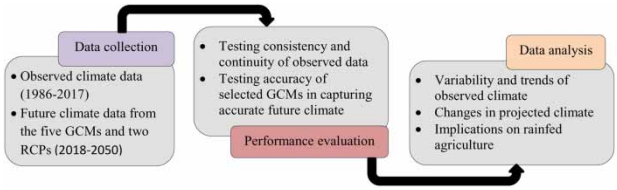

INTRODUCTION

The world's climate has been changing for several thousands of years with a widespread impact on human and natural systems (Kotir 2011; Marohasy *et al.* 2017; Birara *et al.* 2018; Yadav 2018). However, its change has become more rapid and unusual in recent decades relative to that of the past, which can be shown through observations of increasing temperature, sea-level rise, increase in the emission of greenhouse gases (GHGs), frequent floods and droughts, and changes in the amount, distribution and patterns of rainfall (Asare-Nuamah & Botchway 2019). Although climate change is global in its extent and impacts, Africa has been identified as the most vulnerable continent to climate change due to low adaptive capacity and high reliance on climate-sensitive sectors such as rain-fed agriculture (Conway & Schipper 2011; Kotir 2011; Calzadilla *et al.* 2013; Gebrechorkos *et al.* 2019; Girvetz *et al.* 2019). Rainfall variability and warming of temperature are being perceived as the two most important variables of climate change, imposing a crippling effect on the productivity of the agricultural sector and sustainable economic development in Africa, particularly in sub-Saharan African (SSA) countries (Carter & Parker 2009; Conway & Schipper 2011; Calzadilla *et al.* 2013; Serdeczny *et al.* 2017; Abera *et al.* 2018; Asfaw *et al.* 2018; Gebrechorkos *et al.* 2019).

Ethiopia is one of the SSA countries that is extremely vulnerable to the impacts of climate change and variability (Conway & Schipper 2011; Birara *et al.* 2018). Recurrent droughts combined with changes in the amount and spatial distribution of seasonal and annual rainfall are among the major climate-related disasters in Ethiopia (Seleshi & Zanke 2004; Korecha & Barnston 2007; Addisu *et al.* 2015; Zeleke *et al.* 2017; Weldearegay & Tedla 2018), thereby significantly affecting the productivity of rainfed agriculture and the economic and social development of the country. Agriculture is the main sector of the Ethiopian economy supporting about 49% GDP, more than 80% employment, and 80% foreign exchange (CSA 2014). With only about 5% of the total cultivated land being under irrigation (Awulachew & Ayana 2011), agriculture in Ethiopia heavily depends on natural rainfall (Addisu *et al.* 2015). Therefore, any change in the amount and distribution of rainfall would severely threaten agricultural productivity, and have immediate implications for food production and security across the country.

The variability of monsoon rainfall in Ethiopia, mainly in the north-western part of the country, is mostly associated with the El Niño-Southern Oscillation (ENSO) events, the warming of equatorial waters in the Pacific Ocean (Korecha & Barnston 2007; Richman *et al.* 2016). The warming of the ocean temperature leads to the variation in pattern and distribution of rainfall, particularly that of monsoon or summer rain, and changes the direction of the Inter-Tropical Convergence Zone (ITCZ) by altering wind pattern and moisture fluxes (Kotir 2011). According to Gleixner *et al.* (2017), ENSO events combined with sea surface temperature (SST) anomalies in the Southern Atlantic and Indian Oceans significantly affect the rainfall distribution in Ethiopia by displacing and weakening the rain-producing air mass. This evidence provides a picture of how Ethiopia is highly exposed to changes and variations in rainfall and temperature at varying space and time. It has also been predicted that increasing rainfall and surface temperature in most of the East African countries will highly affect the availability of water and agriculture in Ethiopia (Fentaw

Downloaded from http://iwa.silverchair.com/jwcc/article-pdf/12/4/1229/896416/jwc0121229.pdf
by guest

et al. 2018; Muhati *et al.* 2018). To this end, a clear understanding of the temporal trends and spatial distribution of past and projected rainfall and temperature is crucial for proper planning and decision making. As the government of Ethiopa strives to expand agricultural production, reliable and timely climate change information is essential for planning and formulation of appropriate mitigation mechanisms.

While several studies have been conducted on observed climatic varability in many parts of Ethiopia (Bewket & Conway 2007; Wagesho *et al.* 2013; Degefu & Bewket 2014; Addisu *et al.* 2015; Asfaw *et al.* 2018; Birara *et al.* 2018; Mekonnen *et al.* 2018), scant evidence is available on future rainfall and temperature projections and change analysis using CMIP5 dataset. The earlier studies on climate variability and changes in Ethiopia have also been focused either on regional or national levels (e.g. Seleshi & Zanke 2004; Korecha & Barnston 2007; Segele *et al.* 2009; Jury 2010; Jury & Funk 2013; Fazzini *et al.* 2015; Gleixner *et al.* 2017; Lewis 2017) putting less emphasis on local scale or catchment-level climate analysis. Local scale studies on climate trends and their implications are imperative to provide valuable guidance for policymakers on how to prepare for climate change adaptation and mitigation, better use and management of water resources, and agricultural developments. Therefore, the main aim of this study is to understand and analyse the variability and changes of past and future temperature and rainfall conditions and their implications for rainfed agriculture in the Rib watershed, northwestern highland Ethiopia. The specific objectives include: (1) to assess the variability and trends of rainfall and temperature over the last few decades; (2) to project the rainfall and temperature changes in the next few decades; and (3) to analyze the possible impact of climate variability and changes on the rain-fed agriculture in the Rib watershed.

STUDY AREA

The Rib watershed is located in north-western highland Ethiopia between 11°40′ and 12°20′ north latitude and 37°30′ and 38°20′ east longitude with a drainage area of 1,975 km^2. The area is characterized by irregular topography, valleys, and gorges with elevation ranging from 1,758 m in the western part of the watershed to over 4,100 m in the south-eastern part (Mount Guna Massif) (Figure 1). This diversity in topography enables the watershed to receive adequate rainfall to satisfy crop water demand and produce different crops and livestock. The mean annual rainfall in the watershed is about 1,503 mm, with a mean annual temperature of 15.6 °C. The climate of the watershed can be divided into three seasons: summer or main rainy season, locally known as *Kiremt* season (June–September), dry or *Bega* season (October–February), and short rainy or *Belg* season (March–May). The rainfall in the study area is generally erratic and unevenly distributed with more than 80% of rainfall occurring during the main rainy season. The agriculture of the watershed is characterized by mixed crop-livestock systems. The major crops grown include maize, barley, wheat, beans, and rice.

DATASETS AND METHODOLOGY

The long-term monthly rainfall and temperature data for both current and future timescales were considered in this study. The daily precipitation and temperature records for twelve weather stations located within and around the Rib watershed were obtained from the National Meteorological Agency (NMA) of Ethiopia for the period 1986–2017. After testing the consistency, spatial representativeness, and continuity of data for each station, only six stations (Deberetabor, Kimirdingay, Yifag, Alember, Gassay, and Addiszemen), which have a relatively long period of data (at least 30 years) and have no more than 10% missing values, were selected and used for further analysis. Table 1 shows the location of the selected stations and their data values.

The future climate projections and analysis were carried out based on the output of five global climate models (GCMs) (i.e. HadGEM2-ES, BCC-CSM1-1, NorESM1-M, MIROC5, and GFDL-ESM2M) derived from the CMIP5 archive under two representative concentration pathway (RCP) scenarios, RCP4.5 and 8.5. RCP4.5 and 8.5 were purposely selected in order to determine the future climate of the area under moderate and extreme greenhouse gas concentration conditions, respectively. The GCMs and RCPs selected in this study have been also considered in previous studies in Ethiopia (Alemseged & Tom 2015; Abera *et al.*

Downloaded from http://iwa.silverchair.com/jwcc/article-pdf/12/4/1229/896416/jwc0121229.pdf
by guest

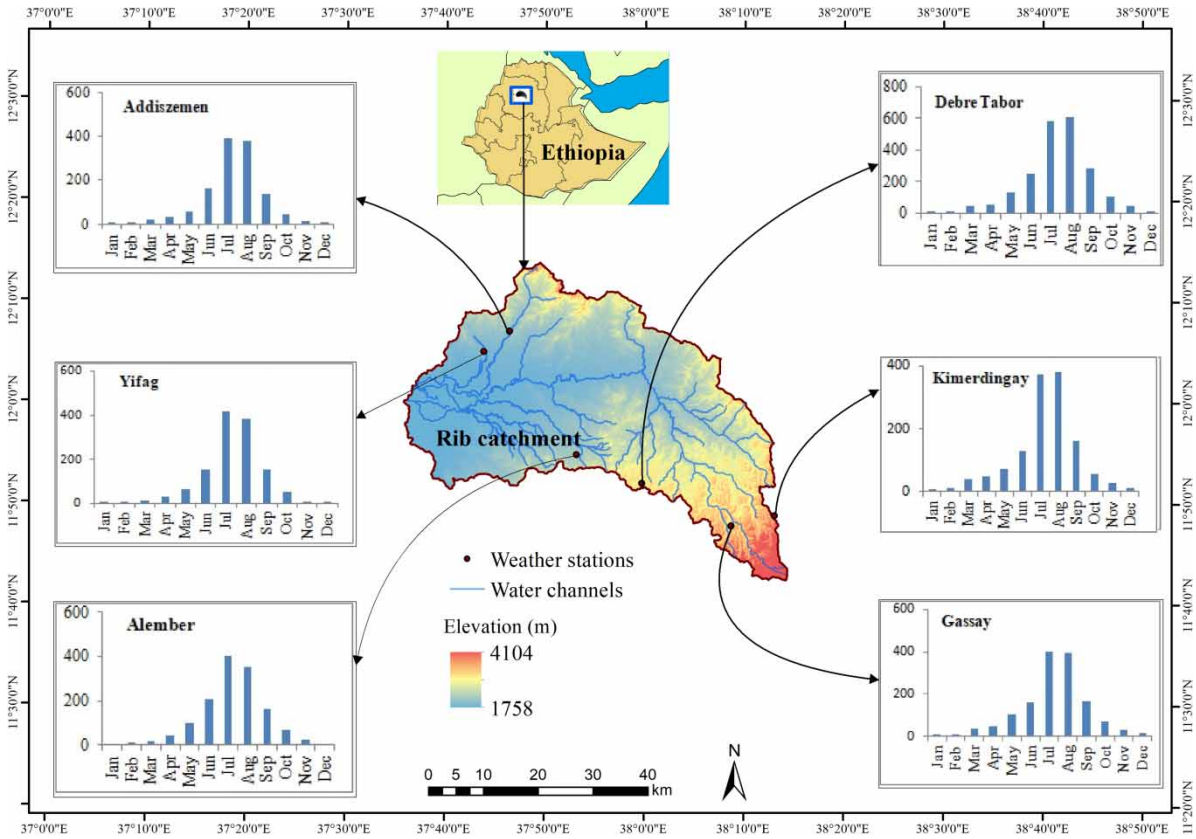

Figure 1 | Location map of the study area and weather stations. For the monthly rainfall graph of each station, the x-axis indicates months, and the y-axis belongs to total rainfall.

Table 1 | Characteristics of stations for recorded rainfall and temperature (1986–2017)

				Rainfall data		Temperature data	
Station	**Lat. (N)**	**Long. (E)**	**Alt. (m)**	**Period**	**Missing value (%)**	**Period**	**Missing value (%)**
Debretabor	11.87	37.99	2,602	1973–2017	0.0	1986–2017	0.8
Gassay	11.79	38.14	2,787	1986–2017	2.7	1986–2017	3.6
Yifag	12.08	37.73	1,850	1978–2017	5.1	1986–2017	3.8
Alember	11.91	37.88	2,043	1986–2017	0.8	1976–2017	1.5
Addiszemen	12.11	37.77	1,931	1974–2017	4.2	1984–2017	7.7
Kimirdingay	11.81	38.21	2,987	1986–2017	3.6	1986–2017	5.2

2018; Bekele *et al.* 2018; Worku *et al.* 2018) and proved to be the best models and scenarios capable of predicting an accurate future climate. The downscaled products of the five models for the period from 2018 to 2050 were downloaded from the MarkSim data distribution center. Although MarkSim has been extensively tested (Jones & Thornton 2013), we assessed the performance of the models by comparing their simulated products (1986–2017) with observed data of the same period using statistical measures such as root mean square error (RMSE), correlation coefficient, bias, and coefficient of variation (CV).

Root mean square error

The RMSE was used to evaluate the difference between observed and simulated rainfall data where the values

Downloaded from http://iwa.silverchair.com/jwcc/article-pdf/12/4/1229/896416/jwc0121229.pdf
by guest

close to zero indicate good performance and vice versa for large values. The RMSE has been regularly employed in many model evaluation studies and verified as the most appropriate standard metric for model errors. We calculated the RMSE using the following equation (Alemseged & Tom 2015; Worku *et al.* 2018):

$$RMSE = \sqrt{\frac{\sum_{t=1}^{N} (R_{Sim} - R_{Obs})^2}{N}} \quad (1)$$

where R_{sim} and R_{obs} denote the simulated and observed rainfall data, respectively, and N represents the analysis period (32 years).

Coefficient of variation

The temporal variability in the annual and seasonal rainfall was assessed using the CV. The CV was used to measure the dispersion of seasonal and annual rainfall from the mean values. It represents the ratio of the standard deviation to the mean and can be computed using the following formula:

$$CV = \frac{\sigma}{\mu} \times 100 \quad (2)$$

where σ is the standard deviation, and μ is the mean rainfall for the chosen timescale. The high values of CV indicate high variability of rainfall and vice versa. According to Asfaw *et al.* (2018), the degree of the variability of rainfall events can be classified into three groups based on the CV values: low (CV < 20), moderate (20 < CV < 30), and high (CV > 30).

Bias

Bias was used to measure how far off the model simulated rainfall is from the observed rainfall, i.e. to measure the volumetric difference between the two datasets. Bias value of zero indicates no systematic difference between simulated and observed rainfall amounts while large values suggest a large deviation. Bias is expressed as (Alemseged & Tom 2015; Worku *et al.* 2018):

$$Bias = 100 \times \frac{\overline{R_{Sim} - R_{Obs}}}{\overline{R_{Obs}}} \quad (3)$$

where R_{sim} and R_{obs} denote the simulated and observed rainfall data, respectively, and the bar over the variables denotes the average over the analysis period (1986–2017).

Correlation coefficient

The correlation coefficient (r) is commonly used to measure the linear relationship between the observed and simulated rainfall. The r values of –1 and 1 indicate perfect alignment between the observed and simulated rainfall, while a value of 0 indicates the absence of a linear relationship. The r can be calculated using the following formula (Alemseged & Tom 2015; Worku *et al.* 2018):

$$r = \frac{\sum_{t=1}^{N} (R_{Sim} - \overline{R_{Sim}})(R_{Obs} - \overline{R_{Obs}})}{\sqrt{\sum_{t=1}^{N} (R_{Sim} - \overline{R_{Sim}}) \sum_{t=1}^{N} (R_{Obs} - \overline{R_{Obs}})}} \quad (4)$$

where R_{sim} and R_{obs} denote the simulated and observed rainfall data, respectively, N represents the analysis period (32 years), and the over-bar symbol denotes the mean statistical operation over the analysis period (1986–2017).

Table 2 indicates the statistical metrics test results of the performance of the selected GCMs in capturing the mean annual rainfall of the Rib watershed. The results confirmed that all the selected models performed well in capturing accurate future rainfall compared to the observed rainfall, but to varying extents. The CV of observed mean annual rainfall was found to be 15.85%, indicating low dispersion of annual rainfall from the mean. The CV values computed

Table 2 | Performance evaluation of the selected models for simulating mean annual rainfall in the Rib watershed, using baseline data from 1986 to 2017

	RMSE (mm/year)	CV (%)	Correlation (r)	Bias (%)
Gauged data	–	15.85	–	–
GFDL-ESM2M	298	22.33	0.299	–12.97
NorESM1-M	384	23.66	0.872	27.58
BCC-CSM1-1	254	24.84	0.038	21.55
HadGEM2-ES	166	16.52	0.563	8.45
MIROC5	465	18.38	0.257	–11.72
Ensemble	373	24.41	0.348	23.85

Downloaded from http://iwa.silverchair.com/jwcc/article-pdf/12/4/1229/896416/jwc0121229.pdf
by guest

for the selected models, particularly those of HadGEM2-ES and MIROC5, also showed a small dispersion of annual rainfall from their mean values. The rainfall values simulated by the GCMs also revealed a positive and high correlation with the observed rainfall ($r > 0.26$). Although no important biases were detected in all models, two models (GFDL-ESM2M and MIROC5) underestimated the annual rainfall in relation to the observed rainfall, whereas the remaining three models and the Ensemble mean overestimated the annual rainfall. Based on the RMSE test, among the evaluated models, HadGEM2-ES performed best (RMSE = 116 mm/year) followed by the BCC-CSM1-1 model (RMSE = 254 mm/year).

Precipitation concentration index

Oliver's (1980) Precipitation Concentration Index (PCI) was used to assess the seasonal and annual variability of rainfall in the study area. The PCI measures the temporal distribution of monthly rainfall and helps to assess the seasonal precipitation changes (Zhang *et al.* 2019). The calculation and evaluation of the PCI have been carried out based on seasonal and annual rainfall records. For seasonal PCI, out of the three Ethiopia seasons (*kiremt*, *belg*, and *bega*), we considered only the *kiremt (*June–September*)* and *belg* (March–May) seasons which are the main sources of rain in the watershed. The PCI for the seasonal and annual scales was calculated using the following formulae (De Luis *et al.* 2011; Birara *et al.* 2018; Alemu & Bawoke 2019; Worku *et al.* 2019):

$$PCI_{annual} = \frac{\sum_{i=1}^{12} pi^2}{\left(\sum_{i=1}^{12} pi\right)^2} \times 100 \quad (5)$$

$$PCI_{kiremt} = \frac{\sum_{i=1}^{4} pi^2}{\left(\sum_{i=1}^{4} pi\right)^2} \times 33.3 \quad (6)$$

$$PCI_{belg} = \frac{\sum_{i=1}^{3} pi^2}{\left(\sum_{i=1}^{3} pi\right)^2} \times 25 \quad (7)$$

where pi denotes the monthly precipitation in the month i. The constant multiplier of 33.3 indicates the share of rainfall that occurred in four months (June–September) out of the 12 months' total rainfall (i.e. 33.3% *kiremt* rain out of the 100% total annual rainfall) and, similarly, 25 infers the rainfall that occurred in three months (March–May), i.e. 25% of the total annual rainfall. Since the rainfall in the study area commonly occurs during the *kiremt* and *belg* seasons, the bega season (dry period) was not considered in the analysis. The calculated PCI values were finally interpreted based on a suggestion by Oliver (1980). He suggested that a PCI value <10 represents a uniform rainfall distribution (low rainfall concentration), values from 11 to 15 indicate moderate rainfall concentration, values from 16 to 20 show irregular rainfall distribution, and PCI > 20 indicate strong irregularity of rainfall distribution (very high concentration).

Mann–Kendall (MK) test

The long-term annual temperature trends across the watershed were analyzed using the MK test and Sen's slope estimator (ß). The non-parametric MK test (Kendall 1975) was used to characterize the trends of the PCI. Since it is less sensitive to outliers and does not require the data to be normally distributed, the MK test is widely used for detecting trends in climatological and hydrological time series analysis data (Birara *et al.* 2018; Panda & Sahu 2019). The MK test statistic '*S*' is calculated as follows:

$$S = \sum_{k=1}^{n-1} \sum_{j=k+1}^{n} \mathrm{sgn}(x_j - x_k), \ where$$
$$\mathrm{sgn}(x_j - x_k) = \begin{cases} +1 & if \quad x_j - x_k > 0 \\ 0 & if \quad x_j - x_k = 0 \\ -1 & if \quad x_j - x_k < 0 \end{cases} \quad (8)$$

where x_j and x_k are the sequential data values of the time series in the years j and k ($j > k$), and n is the length of the time series. In cases where the sample size is greater than 10 ($n > 10$), the statistic '*S*' is approximately normally distributed with mean, and '*S*' becomes zero (Kendall 1975). In this case, the variance statistic is given by:

$$VAR(S) = \left[n(n-1)(2n+5) - \sum_{p=1}^{q} t_p(t_p-1)(2t_p+5)\right] \quad (9)$$

where n is the number of observations, q is the number of tied groups, and t_p is the number of data values in the pth group. Then, the values of '*S*' and '*VAR(S)*' are used to

Downloaded from http://iwa.silverchair.com/jwcc/article-pdf/12/4/1229/896416/jwc0121229.pdf
by guest

compute the test statistic 'Z' as follows:

$$Z = \begin{cases} \dfrac{S-1}{\sqrt{VAR(S)}}, & if \quad S < 0 \\ 0, & if \quad S = 0 \\ \dfrac{S+1}{\sqrt{VAR(S)}}, & if \quad S > 0 \end{cases} \tag{10}$$

where the test statistic Z follows a normal distribution, the positive and negative values of Z indicate the increasing and decreasing trends, respectively. The presence of a statistically significant trend was evaluated using Z values at 5 and 10% significance levels.

Sen's slope estimator

A non-parametric method known as Sen's slope estimator (Sen 1968) was used to determine the magnitude of the trend in the time series. Sen's slope ($ß$) method can be used in cases where the trend can be assumed to be linear (Partal & Kahya 2006). The positive and negative values of $ß$ indicate the increasing and decreasing trend, respectively. The $ß$ of the N pairs of data is computed as (Partal & Kahya 2006):

$$Q_i = \frac{xj - xk}{j - k} \quad for \quad i = 1, 2, 3 \cdots, N \tag{11}$$

where xj and xk are data values at times j and k $(j > k)$, respectively. The median of these 'N' values of Q_i is Sen's estimator of slope and is calculated using the following formula:

$$\beta = \frac{1}{2}\left[\frac{QN}{2} + \frac{Q(N+2)}{2}\right], \ if\ N\ if\ odd\ and$$
$$\beta = \frac{Q(N+1)}{2}, \ if\ N\ is\ even \tag{12}$$

We used a Microsoft Excel add-in software program called XLSTAT to compute the trend and magnitude of change in rainfall and temperature. The spatial distributions and patterns of annual and seasonal rainfall were determined using the inverse distance weighted (IDW) interpolation method in ArcGIS 10.3. The IDW, the reverse function of each point from neighboring points (Teegavarapu & Chandramouli 2005), is among the widely used interpolation techniques which estimate values at unsampled points by the weighting average of observed data at surrounding points (Ly *et al.* 2011).

RESULTS

Variability and trends of observed rainfall

The seasonal and annual variability of rainfall in the watershed was analyzed using the CV and PCI. Table 3 summarizes the results of seasonal and annual rainfall variability across the Rib watershed over the past few decades. The mean rainfall for *Kiremt* season varies from 881 to 1,214 mm while the mean *Belg* rainfall varies from 84 to 184.6 mm. This shows that much of the rainfall in the watershed comes during the *Kiremt* season (June–September), which contributes more than 80% of the rainfall. Most of the analyzed stations show moderate to high seasonal rainfall variations. As shown in Table 3, the *Kiremt* season shows relatively lower variability and low concentration of rainfall compared to that of *Belg* and annual periods.

The trends in annual and seasonal rainfall were assessed by applying Sen's slope and MK tests at 5 and 10% levels of

Table 3 | Seasonal and annual variability of rainfall in the Rib watershed (1986–2017)

	***Belg* season**								
Station	**Mean**	**CV%**	**PCI**	**Mean**	**CV%**	**PCI**	**Mean**	**CV%**	**PCI**
Debretabor	1,214	28.50	8.75	167.62	42.13	21.67	1,514	13.30	19.21
Gassay	1,125	28.00	9.31	184.63	39.52	20.54	1,478	26.00	19.37
Yifag	881	24.70	10.08	84.07	47.40	20.97	1,017	14.40	22.84
Alember	1,065	21.20	7.47	138.24	54.06	24.49	1,326	32.00	21.48
Addiszemen	997	30.60	11.82	108.51	37.74	23.00	1,259	29.00	22.63
Kimerdingay	1,039	46.80	9.66	158.72	49.41	18.68	1,321	15.21	19.75

Downloaded from http://iwa.silverchair.com/jwcc/article-pdf/12/4/1229/896416/jwc0121229.pdf
by guest

significance (Table 4). The annual and *kiremt* rainfall trend analysis results show an increasing trend at four stations out of the total six, whereas the *Belg* rainfall showed a declining trend at four stations. Most of the trends detected for both annual and seasonal rainfall were statistically insignificant at the 5 and 10% levels of significance. The maximum statistically significant increase for annual rainfall was observed at Debretabor station (4.98 mm/year, at a 10% level of significance), whereas a statistically significant maximum increase for *Kiremt* rainfall was 3.95 mm/year observed at Addiszemen station.

The spatial distributions of the annual and seasonal rainfall and their PCI values are shown in Figure 2, indicating high spatial variability in rainfall amounts and concentrations. For both annual and seasonal scales, the southern parts of the watershed receive a significant amount of rainfall while the northern and north-western parts of the watershed receive a relatively lower amount of rainfall. On an annual scale, precipitation concentration in the Rib watershed can be described as strongly irregular on the northern and north-western and uniform on the southern and south-eastern parts. For both annual and seasonal scales, we noticed that the highest values of PCI belong to less rainfall receiving areas, implying more rainfall irregularity in small rainfall receiving areas compared to that of high rainfall receiving areas.

Variability and trends of observed temperature

The changes in long-term minimum, maximum and mean monthly and annual temperatures were analyzed to detect the variabilities and trends across the watershed for the period 1986–2017. The results of descriptive statistics of monthly minimum, maximum, and mean temperature calculated for the average of six stations are summarized in Table 5. The results indicate that the monthly temperature in the watershed has exhibited significant variation during the last few decades. The temperature in the watershed was relatively low during the monsoon season (June–September) and high during pre- and post-monsoon months.

Table 6 summarizes the trends of the annual minimum, maximum and mean temperature in the study area. The increasing trends of temperature were detected for all stations although most of the trends are statistically insignificant at 5 and 10% levels of significance.

Table 4 | Summary statistic of MKs test (Zmk) and Sen's slope estimator (ß) of seasonal and annual rainfall (1986–2017)

	Kiremt		Belg		Annual	
Station	**Zmk**	**ß**	**Zmk**	**ß**	**Zmk**	**ß**
Debretabor	0.36*	2.28	–0.31	–0.13	0.31**	4.98
Gassay	–1.82	–0.55	–1.22*	–0.2	–1.09	–5.33
Yifag	–0.74	–0.97	–0.08**	–0.83	–2.05	–1.45
Alember	0.28	1.47	–0.34	–2.43	0.34*	1.59
Addiszemen	0.22**	3.95	0.57*	0.58	1.38	2.81.9
Kimerdingay	0.47	2.82	1.52	0.2	0.27	3.64

*, **significant at 5 and 10% levels of significance, respectively.

Change in projected rainfall

Projected changes in rainfall and temperature until the middle (2050) of the 21st century under RCP4.5 and 8.5 were analyzed based on the outputs of the five most commonly used GCMs. The projected mean annual and seasonal rainfall for the year 2050 is presented in Figure 3. The mean annual rainfall projected under RCP4.5 varies from 1,386 mm (BCC-CSM1-1) to 1,828 mm (GFDL-ESM2M), whereas mean annual rainfall under RCP8.5 varies from 1,466 to 2,028 mm. For model ensemble, the mean annual rainfall over the whole watershed varies from 1,546 mm (RCP4.5) to 1,718 mm (RCP8.5). With ensemble models, the projected mean *Kiremt* rainfall varies from 1,265 mm (RCP4.5) to 1,317 mm (RCP8.5), whereas the *Belg* rainfall varies from 134 mm (RCP4.5) to 129 mm (RCP 8.5).

The percentage changes in projected annual and seasonal rainfall were computed relative to the baseline rainfall, the rainfall during the observed period (1986–2017). The computed results show that the rainfall in the Rib watershed is expected to increase for both RCPs (Figure 4). Under RCP4.5, the projected change in mean annual rainfall varies from +5.06 (BCC-CSM1-1) to +38.57% (GFDL-ESM2M), whereas the change in mean annual rainfall under RCP8.5 varies from 11 (BCC-CSM1-1) to 54% (GFDL-ESM2M). For model ensemble, the mean annual rainfall in the future is expected to increase by 17% (RCP4.5) and 30% (RCP8.5). The model ensemble projected

Downloaded from http://iwa.silverchair.com/jwcc/article-pdf/12/4/1229/896416/jwc0121229.pdf
by guest

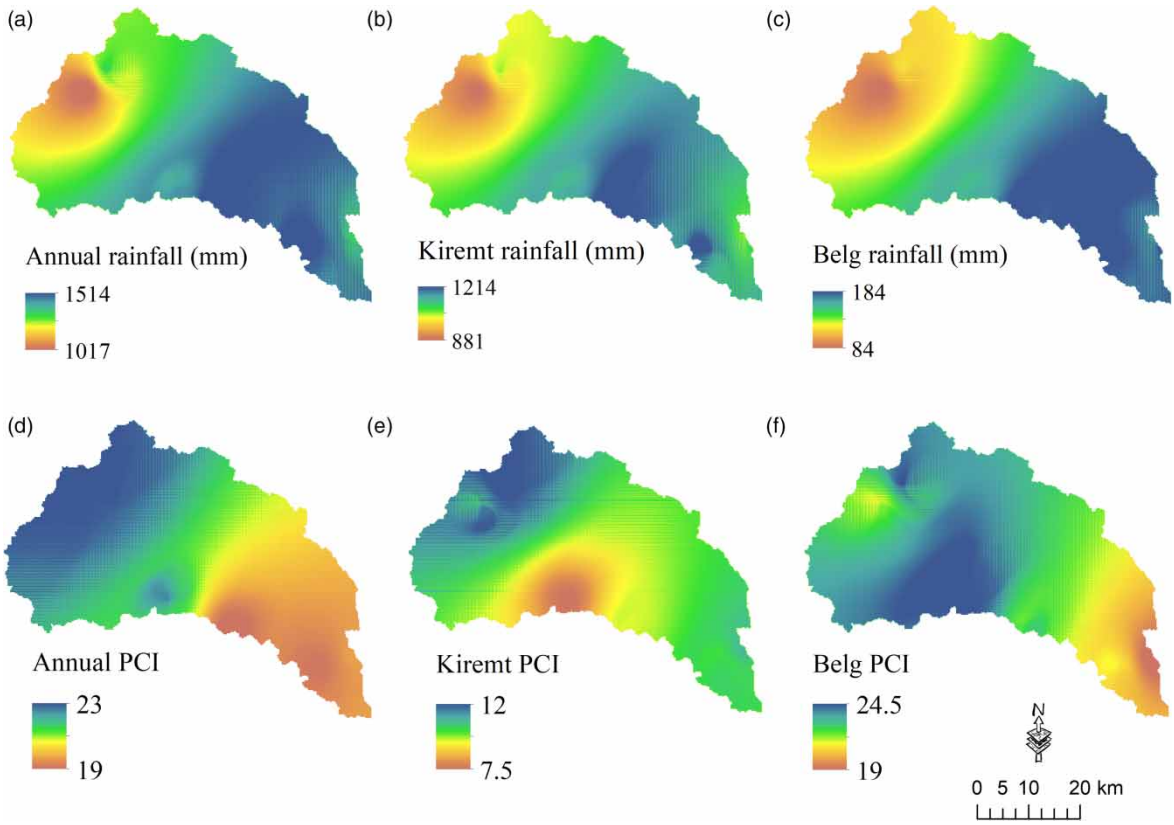

Figure 2 | The spatial distribution of mean annual and seasonal rainfall and PCI values in the Rib watershed during the period 1986–2017: (a) mean annual rainfall, (b) mean *Kiremt* rainfall, (c) mean *Belg* rainfall, (d) PCI values for annual rainfall, (e) PCI values for *Kiremt* rainfall, and (f) PCI values for *Belg* rainfall.

Table 5 | Descriptive statistics of monthly temperature variations in the Rib watershed (1986–2017)

Month	Jan	Feb	Mar	Apr	May	Jun	Jul	Aug	Sep	Oct	Nov	Dec
$T_{minimum}$												
Min	5.3	6.6	7.7	8.1	8.6	8.4	8.6	8.6	6.8	4.6	4.8	4.5
Max	10.0	11.5	11.3	13.1	12.8	12.9	12.7	12.1	11.6	11.0	9.4	9.5
SD	2.1	2.1	1.7	2.1	2.0	1.9	1.7	1.5	2.0	2.8	2.2	2.2
Mean	8.3	9.5	10.2	10.7	11.1	10.8	10.4	10.2	9.5	8.5	7.9	7.7
$T_{maximum}$												
Min	22.2	23.7	23.8	23.6	22.4	21.7	18.8	18.9	19.9	20.9	21.5	21.4
Max	30.7	31.8	32.8	31.6	31.3	28.1	26.1	25.0	25.5	29.8	29.3	30.4
SD	4.3	4.1	4.2	3.7	4.5	3.5	3.6	3.2	3.1	4.3	3.9	4.5
Mean	25.9	27.5	27.0	26.2	26.7	24.7	21.9	21.7	22.7	24.8	25.0	25.3
T_{mean}												
Min	12.1	13.4	13.5	13.6	14.9	14.2	13.4	13.3	12.6	11.8	11.6	11.5
Max	20.4	21.7	22.0	21.0	21.9	20.0	18.3	18.1	18.5	19.8	19.3	19.5
SD	3.7	3.7	3.6	3.1	3.4	2.9	2.6	2.4	2.8	3.7	3.5	3.7
Mean	16.7	18.0	18.0	17.9	18.8	16.5	16.1	15.3	15.9	16.4	16.0	16.1

Min, Max, and SD denote minimum, maximum, and standard deviation, respectively.
$T_{minimum}$, $T_{maximum}$, and T_{mean} indicate minimum, maximum and mean temperature, respectively.

Downloaded from http://iwa.silverchair.com/jwcc/article-pdf/12/4/1229/896416/jwc0121229.pdf
by guest

Table 6 | Summary statistic of MKs test (Zmk) and Sen's slope estimator (ß) of annual temperature (1986–2017)

	$T_{minimum}$		$T_{maximum}$		T_{mean}	
Station	**Zmk**	**ß**	**Zmk**	**ß**	**Zmk**	**ß**
Debretabor	2.36	0.032	1.744*	0.039	3.445*	0.041
Gassay	0.06**	0.020	0.691	0.011	0.053	0.033
Yifag	0.72	0.027	0.533	0.026	0.106	0.022
Alember	0.82	0.042	0.526	0.013	0.071	0.027
Addiszemen	0.09	0.031	0.682	0.037	1.004	0.033
Kimerdingay	2.94	0.037	0.691**	0.007	1.052*	0.028

*, **significant at 5 and 10% levels of significance, respectively.
$T_{minimum}$, $T_{maximum}$, and T_{mean} indicate minimum, maximum and mean temperature, respectively.

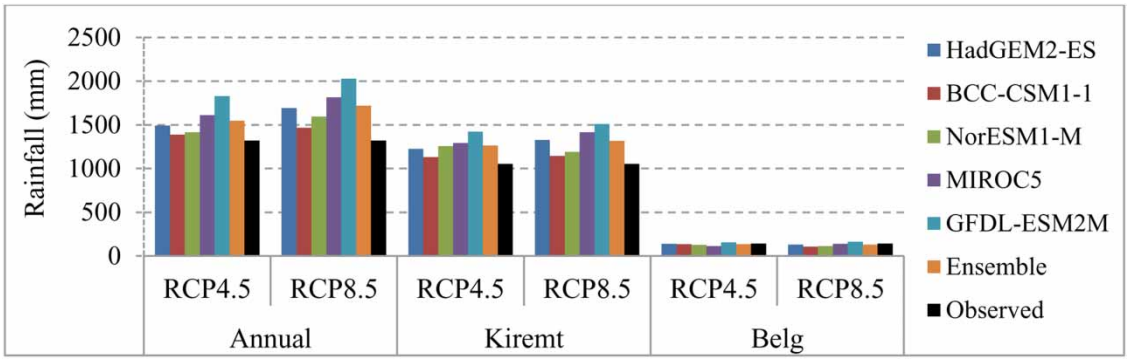

Figure 3 | Projected (2050) annual and seasonal rainfall in the Rib watershed.

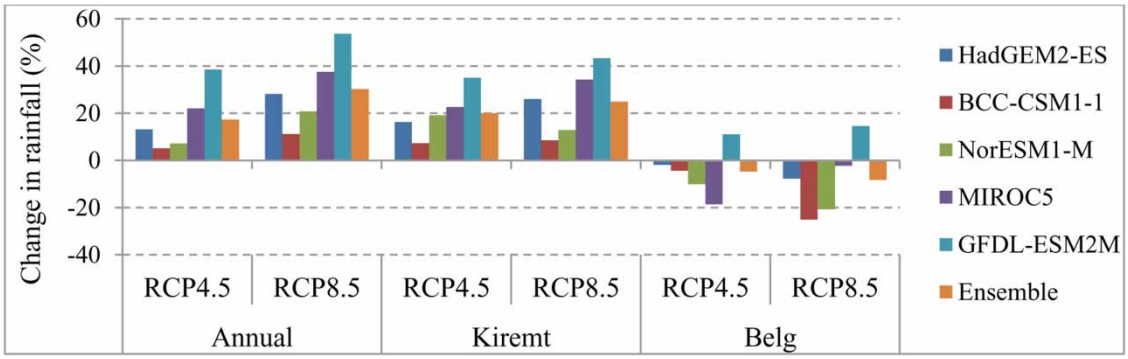

Figure 4 | Changes in projected (2050) mean annual and seasonal rainfall, relative to the baseline period (1986–2017).

about a 20 and 25% increase in *Kiremt* rainfall under RCP4.5 and 8.5, respectively, while the *Belg* rainfall is projected to decline by 4.8 and 8% under RCP4.5 and 8.5, respectively. Except for GFDL-ESM2M, all models predicted decreasing trends in *Belg* rainfall in 2050, compared to the baseline period.

Change in projected temperature

The projection results from the selected model outputs under both scenarios reveal a significant increase in temperature over the Rib watershed in the middle of the 21st century, compared to the baseline period (1986–2017)

Downloaded from http://iwa.silverchair.com/jwcc/article-pdf/12/4/1229/896416/jwc0121229.pdf
by guest

(Figure 5). The projected mean annual minimum temperature ranges from 10.30 °C for GFDL-ESM2M (RCP4.5) to 12.69 °C for NorESM1-M (RCP8.5). On the other hand, the projected mean annual maximum temperature varies from 25.27 °C for GFDL-ESM2M (RCP4.5) to 28.63 °C for NorESM1-M (RCP8.5).

For model ensemble, the minimum temperature is projected to reach 11.12 °C for RCP4.5 and 12.16 °C for RCP8.5 by the middle of the 21st century. The maximum temperature for model ensemble is expected to reach 25.94 and 27.91 °C under mid-range (RCP4.5) and high-range (RCP8.5) scenarios, respectively. Under RCP4.5, the mean temperature for the whole watershed in 2050 is anticipated to reach 18.53 °C and shows a substantial rise to 20.03 °C under RCP8.5. In general, all selected models showed that the temperature projections under RCP8.5 are

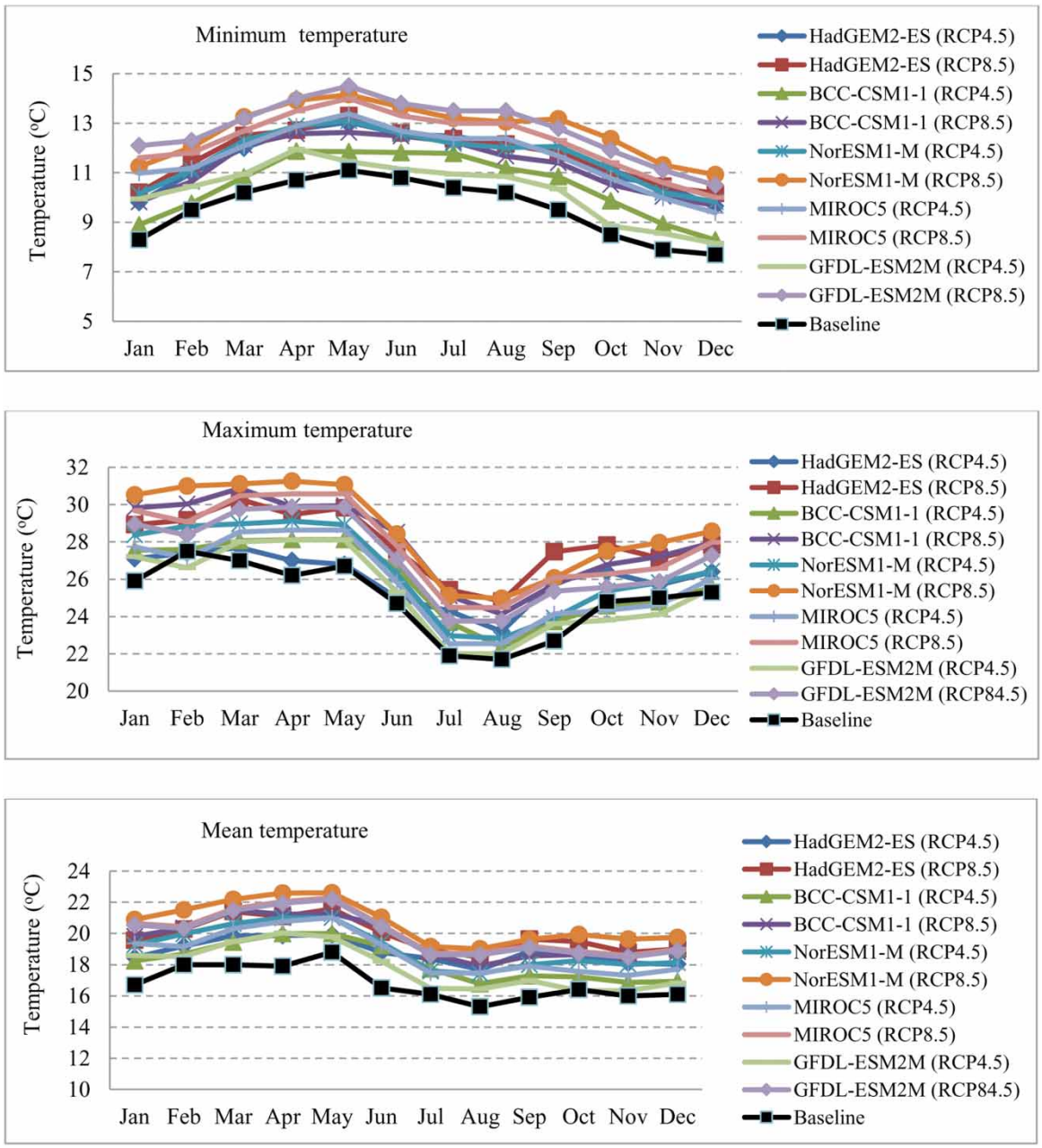

Figure 5 | Projected (2050) temperature in the Rib watershed: (a) minimum temperature, (b) maximum temperature, and (c) mean temperature.

Downloaded from http://iwa.silverchair.com/jwcc/article-pdf/12/4/1229/896416/jwc0121229.pdf
by guest

Table 7 | Changes in projected (2050) mean annual temperature relative to the baseline period (1986–2017)

Model	Tmin		Tmax		Tmean	
	RCP4.5	RCP8.5	RCP4.5	RCP8.5	RCP4.5	RCP8.5
HadGEM2-ES	1.98	2.16	1.13	3.03	1.60	1.61
BCC-CSM1-1	0.92	1.75	0.95	3.05	1.39	2.23
NorESM1-M	2.06	3.12	1.54	3.68	2.25	3.24
MIROC5	2.08	2.70	0.95	2.89	1.96	2.69
GFDL-ESM2M	0.73	3.20	0.42	2.17	1.02	2.66
Ensemble	1.55	2.59	1.00	2.96	1.64	2.49

higher than those of RCP4.5. The rates of change in future temperature were analyzed by comparing the projection results to the baseline period (1986–2017) (Table 7).

The highest mean annual minimum temperature projected under RCP4.5 is 2.08 °C (MIROC5) while the GFDL-ESM2M model under RCP8.5 estimated mean annual minimum temperature is 3.20 °C. For all models, the mean annual maximum temperature shows a significant increase under RCP8.5 compared to that of RCP4.5. The highest mean annual maximum temperature under RCP8.5 is 3.68 °C (NorESM1-M), while the GFDL-ESM2M model estimated the lowest mean annual maximum temperature of 2.17 °C. In general, although the rate of changes in temperature varies across the models and scenarios, projection results show that there is a high certainty of unforeseen increase in minimum and maximum temperature in the watershed by the middle of the 21st century. The increases in temperature will be notably higher under RCP8.5 than that of RCP4.5.

DISCUSSION

Rainfall changes and possible impacts on agriculture

Current records indicate that both seasonal and annual rainfall patterns across the watershed vary extremely and exhibit high temporal and spatial variability. The watershed receives the maximum amount of rainfall in the *Kiremt* season (June–September), particularly in the months of July and August, which alone accounts for more than 50% of the *Kiremt* rainfall. Most parts of the watershed experienced high variability or less reliability of rainfall (CV > 30%) over the last few decades. In all the stations, the CV values of *Belg* rainfall exceed that of *Kiremt* rainfall, implying higher variability of *Belg* rainfall in the watershed than *Kiremt*. Earlier studies (Seleshi & Zanke 2004; Viste *et al.* 2013; Alemayehu & Bewket 2017; Asfaw *et al.* 2018) also indicate more *Belg* rainfall variability than *Kiremt* rainfall in most parts of Ethiopia.

The spatiotemporal distribution of rainfall was also assessed using PCI. On an annual scale, rainfall distribution across the watershed can be described as strongly irregular, as shown by the PCI values exceeding 20. On a seasonal scale, the *Kiremt* was the season where precipitation has been regularly distributed within months (lower PCI values, ranging from 7.5 to 12), while the *Belg* season precipitation distribution was highly irregular (PCI values between 18.5 and 24.5). Birara *et al.* (2018) also found high irregularities in *Belg* rainfall distribution compared to *Kiremt* rainfall in the Tana basin region of Ethiopia. The strong irregularity of annual rainfall distribution observed in the watershed (particularly in the northern and northwestern parts) can be therefore highly attributed to precipitation concentration during the *Belg* season.

The annual and *Kiremt* rainfall shows a general increasing trend at four stations while the *Belg* rainfall shows a decreasing trend at four out of the six stations. However, most of the trends were statistically insignificant at 5 and 10% levels of significance. Previous studies (Alemayehu & Bewket 2017; Asfaw *et al.* 2018) also indicate a statistically insignificant increasing trend of annual and *Kiremt* rainfall and a decreasing trend of *Belg* rainfall in central and north-central highlands of Ethiopia. However, our results contradict earlier studies by Seleshi & Zanke (2004) and Wagesho *et al.* (2013) which reveal decreasing trends of *Kiremt* and annual rainfall in most parts of Ethiopia. This contradiction may be due to the differences in the time period, size of the geographical area studied, number of stations, and data quality and availability (Degefu & Bewket 2014).

Projections based on model ensemble suggested that the *Kiremt* rainfall will probably increase by 20% by 2050 under RCP4.5 and by 25% under RCP8.5 relative to the baseline period (1986–2017). However, the *Belg* rainfall is projected to decline by 4.8 and 8% under RCP4.5 and 8.5, respectively. Our results on future rainfall projections are generally in agreement with previous findings (Hadgu *et al.* 2015; Abera *et al.* 2018; Fentaw *et al.* 2018) which indicate a high

Downloaded from http://iwa.silverchair.com/jwcc/article-pdf/12/4/1229/896416/jwc0121229.pdf
by guest

probability of an increase in annual and *Kiremt* rainfall and a decrease in *Belg* rainfall in different parts of Ethiopia. However, our results contradict previous reports by Arndt *et al.* (2011) and Kassie *et al.* (2014) which show the high possibility of a decline in annual and *Kiremt* rainfall in Ethiopia in the future. According to Emori & Brown (2005) and the IPCC fifth assessment report (IPCC 2013), the dynamic changes in future rainfall would be highly attributed to the human-induced rise of global surface temperature.

Agriculture in highland Ethiopia is predominantly dependent on rainfall. Therefore, any variation in rainfall amount, distribution, and trends will have a direct impact on agricultural production and thus significantly affect the lives of rural smallholder farmers who depend largely on agriculture as their main source of income. A high concentration of rainfall over a few months (July and August) results in more frequent flood events and soil erosion, thereby posing a threat to agricultural production. Flooding and waterlogging in the farmlands significantly reduce crop yield through anaerobic stress in the roots (Fiwa *et al.* 2014), particularly in lower slope areas. Flooding not only inundates the agricultural fields and destroys the crops, but also could highly influence the quality of grazing lands and irrigation facilities at the downstream watershed (Maharjan & Joshi 2013). Excessive rainfall also leads to a high rate of surface runoff and soil erosion that causes the loss of fertile topsoil in the high slope areas and sedimentation in low slope areas in the absence of proper soil conservation structures (O'Neal *et al.* 2005; Fiwa *et al.* 2014; Kassie *et al.* 2014). Loss of soil fertility consequently leads to losses in agricultural production and rural livelihood. Because of the high concentration of rainfall in *Kiremt* season, while other months remain dry or receive little rain, the farmers in the watershed are unable to grow food crops more than once on their small parcel of plots in a given year, which leads to food insecurity and poverty.

A projected increase in annual and seasonal rainfall would have mixed implications for future agriculture in the watershed. On the one hand, an increase in growing season (*Kiremt*) rainfall could considerably contribute to future agriculture under proper soil conservation practices to control associated hazards such as flooding, excessive runoff, and soil loss. On the other hand, unless properly managed, the projected increase in *Kiremt* rainfall will lead to excessive flooding, runoff, and soil loss, thus contributing to a reduction in agricultural yield. High variability and irregular distribution of *Belg* rainfall observed in the watershed could affect not only the agriculture of the *Belg* season but also the agricultural performance of the main rainy season by influencing the early plowing operation and soil moisture availability issues. The declining trend of *Belg* rainfall may also influence the farming practice of the watershed by limiting crop choice and enhancing the loss of biodiversity (Hadgu *et al.* 2015).

Temperature changes and possible impacts on agriculture

Our results show a greater warming trend across the Rib watershed for both current and future scenarios. The mean annual temperature in the study area has increased by 1.07 °C over the last four and a half decades, with an average rate of 0.24 °C per decade. Earlier studies also indicate the occurrence of rapid warming across Ethiopia at varying rates, but consistent with global and African trends. According to Kotir (2011), over the countries lying in the Nile Basin, the mean annual temperature increased in the range of 0.2–0.3 °C per decade during the second half of the 20th century. The studies by Birara *et al.* (2018) and Kassie *et al.* (2014) also show an increasing tendency of temperature in different parts of Ethiopia during the last few decades, with an average rate of between 0.12 and 0.54 °C per decade. Model-based predictions of future climate also clearly suggest the warming of the watershed during the first half of the 21st century. Prediction under model ensemble indicated the rise of average temperature by 1.64 °C (RCP4.5) and 2.49 °C (RCP8.5) in the watershed by the middle of the 21st century, relative to the period (1986–2017). Similar results were found in other parts of Ethiopia, where the future temperature is projected to increase, regardless of the models and emission scenarios used (Conway & Schipper 2011; Kassie *et al.* 2014; Abera *et al.* 2018; Fentaw *et al.* 2018).

The higher increase in growing season temperatures may adversely affect crop production, farm income, and food security in many ways, basically when combined with high inter-annual and intra-seasonal variability of rainfall. The projected warming would reduce the grain yield of

Downloaded from http://iwa.silverchair.com/jwcc/article-pdf/12/4/1229/896416/jwc0121229.pdf
by guest

cereal crops of the watershed which is already experiencing significant reduction due to human-induced soil erosion (Moges & Bhat 2017). A study by Maharjan & Joshi (2013) indicates that an increase in temperature significantly affects mean yield responses as well as yield variability of maize, millet, and sorghum in many African countries. Heat stress reduces grain yield by raising evaporation and reducing water availability (Kang *et al.* 2009; Hatfield & Prueger 2015), particularly in low rainfall receiving downstream areas. It can also cause flower abortion and reproductive failure of crops (Hadgu *et al.* 2015). Moreover, the high temperature could influence crop growth, development, and yield through increased pressure from existing and new pests, weeds, and diseases (Pathak *et al.* 2018). An increase in *Belg* season temperatures can also influence irrigation farming by reducing surface and sub-surface water availability.

The rise in temperature not only influences crop production but also profoundly affects the growth and production patterns of livestock. Heat stress highly affects the productive and reproductive performance of livestock by compromising the reproductive system. An increase in temperature also results in the spread of new and emerging diseases which have a serious effect on livestock productivity and survival (Musemwa *et al.* 2012). The rise in temperature also adversely affects livestock production through competition for natural resources, quality, and quantity of feeds and biodiversity loss while demands for livestock products increase (Garnett 2009).

CONCLUSIONS

This study has presented a detailed analysis of the current and future rainfall and temperature variability and trends in the Rib watershed, north-western highland Ethiopia. A focus has been also given to describe the possible implications of observed and projected climate variability and changes in the farming system of the watershed. The results show that the watershed is highly exposed to spatiotemporal variations in the magnitude and direction of rainfall and temperature. Similar trends of change were found for the current and future rainfall – an increase in annual and *Kiremt* rainfall and a decrease in *Belg* rainfall. Similarly, the analyses of recorded and projected temperature data indicate increasing trends in mean minimum and mean maximum temperature in the study area. The variation in the amount, distribution, and trends of rainfall and warming temperature could have a direct implication for the productivity of rainfed agriculture and the livelihoods of rural farmers who depend largely on agriculture. The observed rainfall and temperature variability and changes would cause excessive runoff and soil loss, exaggerate crop and livestock diseases, and increase evaporation and reduce water availability, thereby significantly influencing agricultural productivity, food security, and rural livelihoods. The findings of the present study would offer useful information to better understand the spatial variability and temporal trends of rainfall and temperature which are essential for water resource management and farming practices.

DATA AVAILABILITY STATEMENT

All relevant data are included in the paper or its Supplementary Information.

REFERENCES

Abera, K., Crespo, O., Seid, J. & Mequanent, F. 2018 Simulating the impact of climate change on maize production in Ethiopia, East Africa. *Environ. Syst. Res.* **7** (4). doi:10.1186/s40068-018-0107-z.

Addisu, S., Selassie, Y. G., Fissha, G. & Gedif, B. 2015 Time series trend analysis of temperature and rainfall in lake Tana Sub-basin, Ethiopia. *Environ. Syst. Res.* **4** (10). doi:1186/s40068-015-0051-0.

Alemayehu, A. & Bewket, W. 2017 Local spatiotemporal variability and trends in rainfall and temperature in the central highlands of Ethiopia. *Geogr. Annal. A Phys. Geogr.* **99**, 85–101. doi:10.1080/04353676.2017.1289460.

Alemseged, T. H. & Tom, R. 2015 Evaluation of regional climate model simulations of rainfall over the Upper Blue Nile basin. *Atmos. Res* **161–162**, 57–64. doi:10.1016/j.atmosres.2015.03.013.

Alemu, M. M. & Bawoke, G. T. 2019 Analysis of spatial variability and temporal trends of rainfall in Amhara region, Ethiopia. *J. Water Clim. Change* jwc2019084, 10.2166/wcc.2019.084.

Arndt, C., Robinson, S. & Willenbockel, D. 2011 Ethiopia's growth prospects in a changing climate: a stochastic general equilibrium approach. *Global Environ. Change* **21**, 701–710. doi:10.1016/j.gloenvcha.2010.11.004.

Asare-Nuamah, P. & Botchway, E. 2019 Understanding climate variability and change: analysis of temperature and rainfall

Downloaded from http://iwa.silverchair.com/jwcc/article-pdf/12/4/1229/896416/jwc0121229.pdf
by guest

across agroecological zones in Ghana. *Heliyon* **5**, e02654. doi:10.1016/j.heliyon.2019.e02654.

Asfaw, A., Simane, B., Hassen, A. & Bantider, A. 2018 Variability and time series trend analysis of rainfall and temperature in northcentral Ethiopia: a case study in Woleka sub-basin. *Weather Clim. Extremes* **19**, 29–41. doi:10.1016/j.wace.2017.12.002.

Awulachew, S. B. & Ayana, M. 2011 Performance of irrigation: an assessment at different scales in Ethiopia. *Exp. Agric.* **47**, 57–69. doi:10.1017/S0014479710000955.

Bekele, D., Alamirew, T., Kebede, A., Zeleke, G. & Melesse, A. M. 2018 Modeling climate change impact on the hydrology of Keleta Watershed in the Awash River Basin, Ethiopia. *Environ. Model. Assess.* **24**, 95–107. doi:10.1007/s10666-018-9619-1.

Bewket, W. & Conway, D. 2007 A note on the temporal and spatial variability of rainfall in the drought-prone Amhara region of Ethiopia. *Int. J. Climatol.* **27**, 1467–1477. doi:10.1002/joc.1481.

Birara, H., Pandey, R. P. & Mishra, S. K. 2018 Trend and variability analysis of rainfall and temperature in the Tana basin region, Ethiopia. *J. Water Clim. Change* **9** (3), 555–569. jwc2018080, 10.2166/wcc.2018.080.

Calzadilla, A., Zhu, T., Rehdanz, K., Tol, R. S. J. & Ringler, C. 2013 Economywide impacts of climate change on agriculture in Sub-Saharan Africa. *Ecol. Econ.* **93**, 150–165. doi:10.1016/j.ecolecon.2013.05.006.

Carter, R. C. & Parker, A. 2009 Climate change, population trends and groundwater in Africa. *Hydrol. Sci. J.* **54**, 676–689. doi:10.1623/hysj.54.4.676.

Conway, D. & Schipper, E. L. F. 2011 Adaptation to climate change in Africa: challenges and opportunities identified from Ethiopia. *Global Environ. Change* **21**, 227–237. doi:10.1016/j.gloenvcha.2010.07.013.

CSA 2014 *The Federal Democratic Republic of Ethiopia Statistical Abstract for 2013*. Addis Ababa, Ethiopia.

Degefu, M. A. & Bewket, W. 2014 Variability and trends in rainfall amount and extreme event indices in the Omo-Ghibe River Basin, Ethiopia. *Reg. Environ. Change* **14**, 799–810. doi:10.1007/s10113-013-0538-z.

De Luis, M., González-Hidalgo, J. C., Brunetti, M. & Longares, L. A. 2011 Precipitation concentration changes in Spain 1946–2005. *Nat. Hazards Earth Syst. Sci.* **11**, 1259–1265. doi:10.5194/nhess-11-1259-2011.

Emori, S. & Brown, S. J. 2005 Dynamic and thermodynamic changes in mean and extreme precipitation under changed climate: mean and extreme precipitation changes. *Geophys. Res. Lett.* **32**. doi:10.1029/2005GL023272.

Fazzini, M., Bisci, C. & Billi, P. 2015 The Climate of Ethiopia. In: *Landscapes and Landforms of Ethiopia* (P. Billi, ed.). Springer Netherlands, Dordrecht, pp. 65–87. doi:10.1007/978-94-017-8026-1_3.

Fentaw, F., Hailu, D., Nigussie, A. & Melesse, A. M. 2018 Climate change impact on the hydrology of Tekeze Basin, Ethiopia: projection of rainfall-runoff for future water resources planning. *Water Conserv. Sci. Eng.* **3**, 267–278. doi:10.1007/s41101-018-0057-3.

Fiwa, L., Vanuytrecht, E., Wiyo, K. & Raes, D. 2014 Effect of rainfall variability on the length of the crop growing period over the past three decades in central Malawi. *Clim. Res.* **62**, 45–58. doi:10.3354/cr01263.

Garnett, T. 2009 Livestock-related greenhouse gas emissions: impacts and options for policy makers. *Environ. Sci. Policy* **12**, 491–503. https://doi.org/10.1016/j.envsci.2009.01.006.

Gebrechorkos, S. H., Hülsmann, S. & Bernhofer, C. 2019 Long-term trends in rainfall and temperature using high-resolution climate datasets in East Africa. *Sci. Rep.* **9**, 11376. doi:10.1038/s41598-019-47933-8.

Girvetz, E., Ramirez-Villegas, J., Claessens, L., Lamanna, C., Navarro-Racines, C., Nowak, A., Thornton, P. & Rosenstock, T. S. 2019 Future climate projections in Africa: where are we headed? In: *The Climate-Smart Agriculture Papers* (T. S. Rosenstock, A. Nowak & E. Girvetz, eds). Springer International Publishing, Cham, pp. 15–27. doi:10.1007/978-3-319-92798-5_2.

Gleixner, S., Keenlyside, N., Viste, E. & Korecha, D. 2017 The El Niño effect on Ethiopian summer rainfall. *Clim. Dyn.* **49**, 1865–1883. https://doi.org/10.1007/s00382-016-3421-z.

Hadgu, G., Tesfaye, K. & Mamo, G. 2015 Analysis of climate change in Northern Ethiopia: implications for agricultural production. *Theor. Appl. Climatol.* **121**, 733–747. doi:10.1007/s00704-014-1261-5.

Hatfield, J. L. & Prueger, J. H. 2015 Temperature extremes: effect on plant growth and development. *Weather Clim. Extremes* **10**, 4–10. doi:10.1016/j.wace.2015.08.001.

IPCC 2013 *Climate Change 2013: The Physical Science Basis. Contribution of Working Group I to the Fifth Assessment Report of the Intergovernmental Panel on Climate Change*. Cambridge University Press, United Kingdom and New York, USA.

Jones, P. G. & Thornton, P. K. 2013 Generating downscaled weather data from a suite of climate models for agricultural modelling applications. *Agric. Syst.* **114**, 1–5. doi:10.1016/j.agsy.2012.08.002.

Jury, M. R. 2010 Ethiopian decadal climate variability. *Theor. Appl. Climatol.* **101**, 29–40. doi:10.1007/s00704-009-0200-3.

Jury, M. R. & Funk, C. 2013 Climatic trends over Ethiopia: regional signals and drivers: climatic trends over Ethiopia: regional signals and drivers. *Int. J. Climatol.* **33**, 1924–1935. doi:10.1002/joc.3560.

Kang, Y., Khan, S. & Ma, X. 2009 Climate change impacts on crop yield, crop water productivity and food security – a review. *Progr. Nat. Sci.* **19**, 1665–1674. doi:10.1016/j.pnsc.2009.08.001.

Kassie, B. T., Rötter, R. P., Hengsdijk, H., Asseng, S., Van Ittersum, M. K., Kahiluoto, H. & Van Keulen, H. 2014 Climate variability and change in the Central Rift Valley of Ethiopia: challenges for rainfed crop production. *J. Agric. Sci.* **152**, 58–74. doi:10.1017/S0021859612000986.

Kendall, M. G. 1975 *Rank Correlation Methods*, 4th edn. Charles Griffin, London.

Korecha, D. & Barnston, A. G. 2007 Predictability of June–September rainfall in Ethiopia. *Month. Weather Rev.* **135**, 628–650. doi:10.1175/MWR3304.1.

Downloaded from http://iwa.silverchair.com/jwcc/article-pdf/12/4/1229/896416/jwc0121229.pdf
by guest

Kotir, J. H. 2011 Climate change and variability in sub-saharan Africa: a review of current and future trends and impacts on agriculture and food security. *Environ. Dev. Sustainable* **13**, 587–605. doi:10.1007/s10668-010-9278-0.

Lewis, K. 2017 Understanding climate as a driver of food insecurity in Ethiopia. *Clim. Change* **144**, 317–328. doi:10.1007/s10584-017-2036-7.

Ly, S., Charles, C. & Degré, A. 2011 Geostatistical interpolation of daily rainfall at catchment scale: the use of several variogram models in the Ourthe and Ambleve catchments, Belgium. *Hydrol. Earth Syst. Sci.* **15**, 2259–2274. doi:10.5194/hess-15-2259-2011.

Maharjan, K. L. & Joshi, N. P. 2013 *Climate Change, Agriculture and Rural Livelihoods in Developing Countries*. Springer Japan, Tokyo. doi:10.1007/978-4-431-54343-5.

Marohasy, J., Marohasy, J. & Institute of Public Affairs (Australia) 2017 *Climate Change: the Facts 2017*. Connor Court Publishing Pty Ltd., Australia.

Mekonnen, Z., Kassa, H., Woldeamanuel, T. & Asfaw, Z. 2018 Analysis of observed and perceived climate change and variability in Arsi Negele District, Ethiopia. *Environ. Dev. Sustainable* **20**, 1191–1212. doi:10.1007/s10668-017-9934-8.

Moges, D. M. & Bhat, H. G. 2017 Integration of geospatial technologies with RUSLE for analysis of land use/cover change impact on soil erosion: case study in Rib watershed, north-western highland Ethiopia. *Environ. Earth Sci.* **76** (765). doi:10.1007/s12665-017-7109-4.

Muhati, G. L., Olago, D. & Olaka, L. 2018 Past and projected rainfall and temperature trends in a sub-humid Montane Forest in Northern Kenya based on the CMIP5 model ensemble. *Global Ecol. Conserv.* **16**, e00469. doi:10.1016/j.gecco.2018.e00469.

Musemwa, L., Muchenje, V., Mushunje, A. & Zhou, L. 2012 The impact of climate change on livestock production amongst the resource-poor farmers of Third World Countries: a review. *Asian J. Agric. Rural Dev.* **13**, 621–631.

Oliver, J. E. 1980 Monthly precipitation distribution: a comparative index. *Prof. Geogr.* **32**, 300–309. doi:10.1111/j.0033-0124.1980.00300.x.

O'Neal, M. R., Nearing, M. A., Vining, R. C., Southworth, J. & Pfeifer, R. A. 2005 Climate change impacts on soil erosion in Midwest United States with changes in crop management. *Catena* **61**, 165–184. doi:10.1016/j.catena.2005.03.003.

Panda, A. & Sahu, N. 2019 Trend analysis of seasonal rainfall and temperature pattern in Kalahandi, Bolangir and Koraput districts of Odisha, India. *Atmos. Sci. Lett.* **20**. doi:10.1002/asl.932.

Partal, T. & Kahya, E. 2006 Trend analysis in Turkish precipitation data. *Hydrol. Processes* **20**, 2011–2026. doi:10.1002/hyp.5993.

Pathak, T., Maskey, M., Dahlberg, J., Kearns, F., Bali, K. & Zaccaria, D. 2018 Climate change trends and impacts on California agriculture: a detailed review. *Agronomy* **8** (25). doi:10.3390/agronomy8030025.

Richman, M. B., Leslie, L. M. & Segele, Z. T. 2016 Classifying drought in Ethiopia using machine learning. *Proc. Comput. Sci.* **95**, 229–236. doi:10.1016/j.procs.2016.09.319.

Segele, Z. T., Lamb, P. J. & Leslie, L. M. 2009 Seasonal-to-interannual variability of Ethiopia/Horn of Africa monsoon. Part I: associations of wavelet-filtered large-scale atmospheric circulation and global sea surface temperature. *J. Clim.* **22**, 3396–3421. doi:10.1175/2008JCLI2859.1.

Seleshi, Y. & Zanke, U. 2004 Recent changes in rainfall and rainy days in Ethiopia. *Int. J. Climatol.* **24**, 973–983. doi:10.1002/joc.1052.

Sen, P. K. 1968 Estimates of the regression coefficient based on Kendall's Tau. *J. Am. Stat. Assoc.* **63**, 1379–1389. doi:10.1080/01621459.1968.10480934.

Serdeczny, O., Adams, S., Baarsch, F., Coumou, D., Robinson, A., Hare, W., Schaeffer, M., Perrette, M. & Reinhardt, J. 2017 Climate change impacts in Sub-Saharan Africa: from physical changes to their social repercussions. *Reg. Environ. Change* **17**, 1585–1600. doi:10.1007/s10113-015-0910-2.

Teegavarapu, R. S. V. & Chandramouli, V. 2005 Improved weighting methods, deterministic and stochastic data-driven models for estimation of missing precipitation records. *J. Hydrol.* **312**, 191–206. doi:10.1016/j.jhydrol.2005.02.015.

Viste, E., Korecha, D. & Sorteberg, A. 2013 Recent drought and precipitation tendencies in Ethiopia. *Theor. Appl. Climatol.* **112**, 535–551. doi:10.1007/s00704-012-0746-3.

Wagesho, N., Goel, N. K. & Jain, M. K. 2013 Temporal and spatial variability of annual and seasonal rainfall over Ethiopia. *Hydrol. Sci. J.* **58**, 354–373. doi:10.1080/02626667.2012.754543.

Weldearegay, S. K. & Tedla, D. G. 2018 Impact of climate variability on household food availability in Tigray, Ethiopia. *Agric. Food Secur.* **7**. doi:10.1186/s40066-017-0154-0.

Worku, G., Teferi, E., Bantider, A., Dile, Y. T. & Taye, M. T. 2018 Evaluation of regional climate models performance in simulating rainfall climatology of Jemma sub-basin, Upper Blue Nile Basin, Ethiopia. *Dyn. Atmos. Oceans* **83**, 53–63. doi:10.1016/j.dynatmoce.2018.06.002.

Worku, T., Khare, D. & Tripathi, S. K. 2019 Spatiotemporal trend analysis of rainfall and temperature, and its implications for crop production. *J. Water Clim. Change* **10**, 799–817. doi:10.2166/wcc.2018.064.

Yadav, S. S. (ed.). 2018 *Food Security and Climate Change*, 1st edn. John Wiley & Sons, Ltd, Hoboken, NJ, p. 1.

Zeleke, T. T., Giorgi, F., Diro, G. T. & Zaitchik, B. F. 2017 Trend and periodicity of drought over Ethiopia. *Int. J. Climatol.* **37**, 4733–4748. doi:10.1002/joc.5122.

Zhang, K., Yao, Y., Qian, X. & Wang, J. 2019 Various characteristics of precipitation concentration index and its cause analysis in China between 1960 and 2016. *Int. J. Climatol.* **39**, 4648–4658. doi:10.1002/joc.6092.

First received 9 March 2020; accepted in revised form 14 June 2020. Available online 6 August 2020

Downloaded from http://iwa.silverchair.com/jwcc/article-pdf/12/4/1229/896416/jwc0121229.pdf
by guest